The NOνA Experiment, A long-baseline neutrino experiment at the intensity frontier

A.Norman[*][†]

Fermi National Accelerator Laboratory

E-mail: anorman@fnal.gov

NOνA is a second generation, accelerator based, long baseline experiment which has been designed to make precision measurements of neutrino mixing parameters. The experiment has been optimized to simultaneously measure electron neutrino appearance and muon neutrino disappearance rates in a ν_μ beam with a narrow energy spectrum centered around 2 GeV. Recent measurements indicating a non-zero value of the neutrino mixing angle θ_{13} have lead to improved estimates for the ability of the NOνA detector to resolve the neutrino mass hierarchy and probe for CP violation in the neutrino sector. We present these updated sensitivities as well as updates on the NOνA detectors.

The XIth International Conference on Heavy Quarks and Leptons,
June 11-15, 2012
Prague, Czech Republic

---

[*]Speaker.

[†]Department of Energy and Fermi Research Alliance

1. Introduction

Our knowledge of neutrino mixing has changed dramatically over the past year with new results from the Daya Bay[4], Reno[5] and Double Chooz[6] reactor experiments which have indicated a non-zero value for the mixing angle θ_{13} through the electron anti-neutrino disappearance spectrum over a short baseline. At the same time new measurements from the T2K[2] and MINOS[3] experiments have also favored a non-zero θ_{13} through the electron neutrino appearance signature over long baselines. These results when combined through global fits[1] yield a best fit value of θ_{13} such that,

$$\sin^2\theta_{13} = 0.026^{+0.003}_{-0.004}, \tag{1.1}$$

or $\theta_{13} \approx 8.8°$. These new measurements shift the landscape of neutrino oscillations from one where we knew very little about the size of θ_{13} as compared to the former Chooz limit, to one where θ_{13} is well measured. As a result of these measurements the neutrino community is now able to reevaluate the capabilities of long baseline experiments to make measurements that can exploit the mixing in the ν_1/ν_3 sector. Experimentally the goals of many experiments now must shift from trying to measure if θ_{13} is non-zero, to three major programs of study that examine the nature of neutrino flavor.

The first of these programs focuses on the possibility of there being a significant source of CP-violation in the neutrino sector. This program looks to make a series of precision measurements to determine if the Dirac phase δ_{CP} of the PMNS matrix is non-zero. If δ_{CP} is found to be inconsistent with zero, this would indicate a source of CP violation in the neutrino sector and the size of the source would be investigated through improved measurement techniques that are sensitive to the size of δ_{CP}.

The second major experimental program that neutrino community needs to address, is the structure of the neutrino mass states and their relation to the weak, charged current flavor states. Through measurements in the solar and atmospheric sectors, the splittings between mass eigen states of the three active neutrinos have been measured, but the determination of which flavor states correspond to the heaviest and lightest mass eigenstates has yet to be determined. Determination of the sign of the mass splitting Δm^2_{13} would fully constrain the sector and allow us to understand whether the neutrino mass states are ordered similar to the charged leptons, with the state coupling to the electron being the lightest, or whether the neutrinos observe an inverted ordering with the neutrino mass state that couples most to the τ lepton being the lightest. The determination of the sign of this mass splitting requires an experiment with a long enough baseline for the oscillation probabilities to be significantly enhanced or suppressed by matter effects that are sensitive to the sign of the mass splitting.

The third major experimental program is an effort to make precision measurement of all the neutrino mixing parameters to over constrain the standard three flavor mixing model. In over constraining the mixing model, there will be an opportunity to look for the effects of new physics in much the same manner that precision tests of the CKM mixing parameters have probed for physics beyond the standard model.

For the NOνA experiment the relatively large measured value of θ_{13} opens up new possibilities in the measurements of these quantities. In particular NOνA will be able to make new precision measurements of θ_{13}, θ_{23} in both the neutrino and anti-neutrino oscillation modes, constrain the
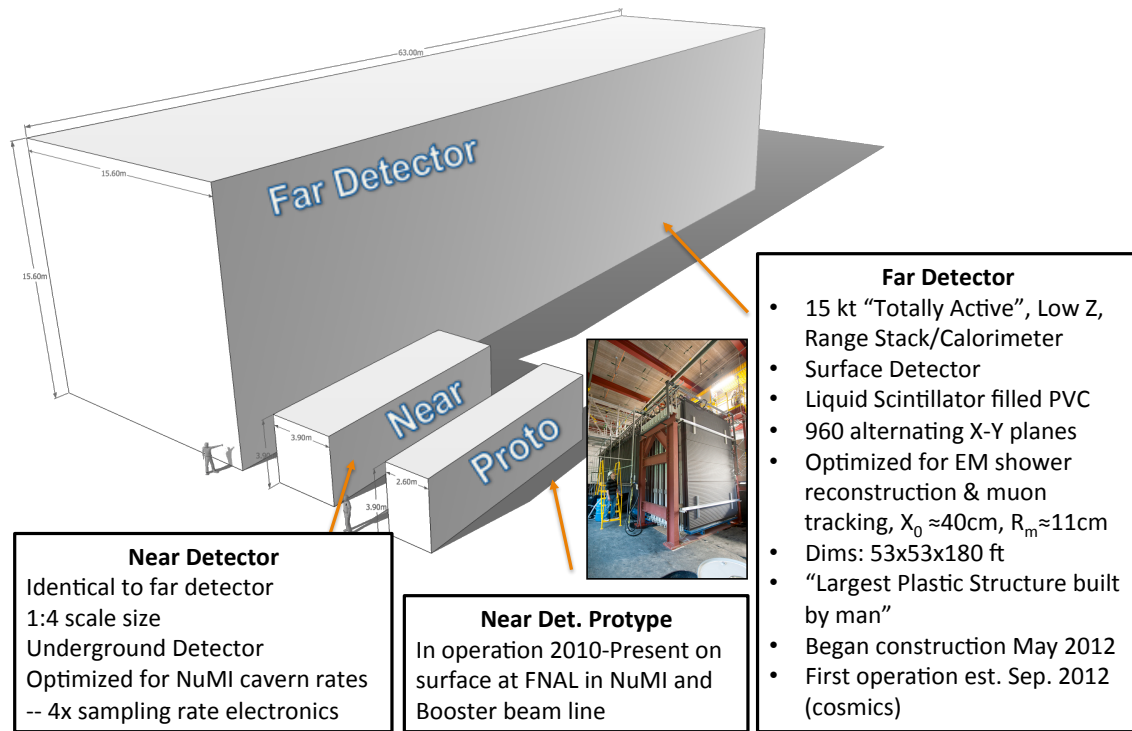
Figure 1: The NOνA experiment will build a total of three separate detectors. The far detector is the largest at a total mass of 15 kT, while the smallest is the near detector prototype which was built in 2010 and operated from the fall of 2010 through May 1, 2012 in the NuMI and Booster neutrino lines at Fermilab.

sign of Δm^2_{13} over a significant portion of the available parameter space in δ_{CP} and measure the quadrant that θ_{23} couples to. These sensitivities are discussed in section 3.

2. The NOνA Detector

The NOνA experiment will build a total of three detectors over the course of the project. The detectors consist of a 15 kt far detector and functionally identical 1/4 size near detector for performing the oscillation measurements. These detectors are shown in Fig. 1. Ind addtion a smaller 200 ton prototype near detector has been built and used for design validation and initial studies in the NuMI and booster neutrino beams at Fermilab. Each of the detectors has been designed as a totally active, highly segmented, low-Z, range-stack/calorimeter. The detector geometry consists of alternating planes of X-measuring and Y-measuring detection cells. The detection planes are created by filling a 15.5 m long ridged plastic (PVC) extrusion, which has been segmented into an and array of 3.9×6.6 cm roughly rectangular profile cells, with a mineral oil based liquid scintillator and a single wavelength shifting fiber that is looped down through the entire length of the cell. Both ends of the fiber are mated through an optical connector to a 32 pixel Avalanche Photo Diode (APD). The APD signals from 32 adjacent detectors cells are sampled through a custom readout board which provides an amplifier, shaper and multiplexed waveform digitizer capable of

continuous digitization at 16 MHz. The resulting data is sparsified through a simple digital signal processing algorithm that is performed in an FPGA on the front end readout board. For hits occurring at the far end of a far detector cell, this results in a single hit signal threshold of approximately 1/2 a MIP, corresponding to 6-8 MeV of visible energy. For the far detector a total of 386,640 individual readout channels each being continuously digitized at an effective rate of 2 MHz form the data stream that is collected by the data acquisition system and passed to a large computing farm at the Ash River complex for buffer and trigger decisions.
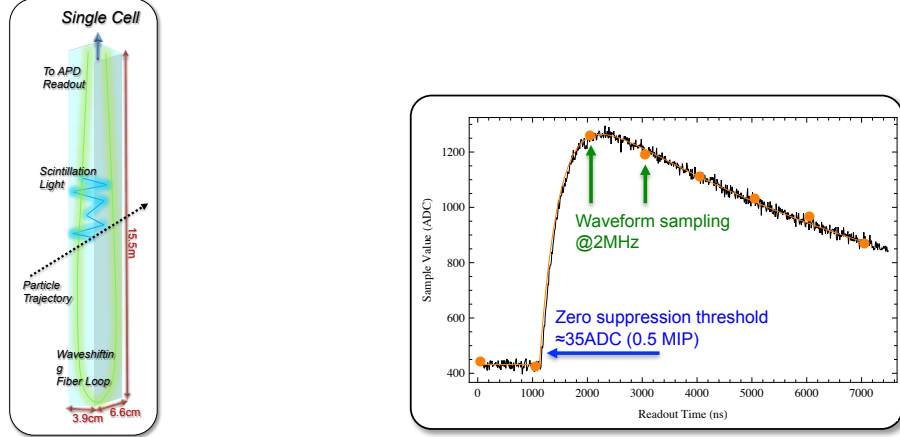
(a) The NOνA readout cell is a 15 m long column of liquid scintillator with a 3.9×6.6 cm cross section.

(b) The response from each detection cell is amplified and shaped by a custom ASIC and then sparsely sampled by a waveform digitizer.

Figure 2: NOνA readout cell and digitization.

The location of the NOνA detectors have been chosen to be in an "off-axis" configuration, where instead of placing the detectors directly on the beam axis, they are instead chosen to be at a small angle θ off of the primary beam axis. In doing so the two body kinematics of the $\pi, K \to \mu \nu_\mu$ decay channels link the neutrino energy to its angle relative to the boost axis according to,

$$E_\nu = \frac{\left(1 - m_\mu^2/m_{\pi,K}^2\right) E_{\pi,K}}{1 + \gamma^2 \theta^2} \quad (2.1)$$

This has the effect of projecting the neutrino energy spectrum down at high parent π, K energies and making the spectrum almost flat across a wide range in energy. In particular, at 14 mrad to the beam axis, the neutrino energy spectrum arising from parent pion decays becomes a narrow band centered around 2 GeV, as shown in Fig. 3. The NOνA experiment takes advantage of this by placing the near and far detectors at this angle and then tuning the far detector baseline to 810 km to place the detector at the first oscillation maximum for a central neutrino energy of 2 GeV. This not only maximized the experiment's sensitivity to the ν_e appearance and ν_μ disappearance signals, but significantly reduces beam related backgrounds coming from higher energy neutral current interactions and reduces the systematic uncertainties related to the knowledge of the π/K ratios and energy spectra coming off of the production target.

Off Axis Neutrino Energy
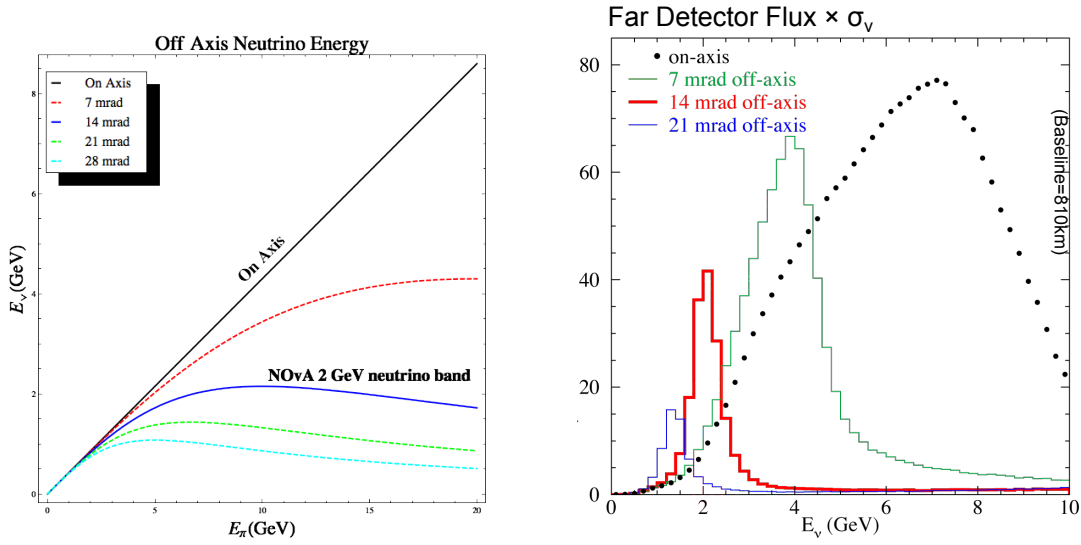
(a) The pion decay kinematics project the energy of neutrinos at 14 mrad into a narrow band around 2 GeV.

Far Detector Flux × σ$_ν$

(b) Far Detector Flux time cross section for the NuMI neutrino beam in both the on-axis and off-axis configurations.

Figure 3: Off-axis neutrino beam configuration for the NOνA experiment

The prototype near detector was similarly chosen to be located in an off-axis location on the Fermilab site. The prototype near detector was placed 112 mrad vertically off of the NuMI beam access in a surface location that also allowed the detector to be exposed to the on-axis Booster neutrino beam. This unique site permitted the detector to see neutrinos in a 2 GeV peak arising from parent kaon decays in the NuMI beam, while also seeing the full energy spectrum of neutrinos from the 8 GeV booster neutrino beam. This "neutrino test beam" configuration allowed the detector to be exposed to different fluxes and beam time structures that have allowed the experiment to characterize the low energy response of the NOνA detector. The prototype near detector ran in this configuration from December 2010 through May 1, 2012. The detector will continue running in this configuration after upgrades to the Fermilab accelerator complex are completed in 2013.

3. Physics Sensitivities

The sensitivities for analyses which depend on the ν_e and $\bar{\nu}_e$ oscillation probabilities are based on the expected event rates that the NOνA experiment will see over the course of its run periods. Table 3 shows the expected ν_e signal events, total background events and the background broken down into its neutral current and charged current components. These rates assume the current global fit value for θ_{13}, $\sin^2 2\theta_{13} = 0.095$. The estimates assume conservative values for signal efficiencies of 41% (ν) and 48% ($\bar{\nu}$) and a total of 18×10^{20} protons on target (POT) over three years each of neutrino and anti-neutrino running. In computing the sensitivities of the experiment a 10% uncertainty was added to the backgrounds.

Beam	Signal	NC Bkg	ν_μ CC	ν_e CC	Total Bkg
ν (3 yr)	72.6	20.8	5.2	8.4	34.5
$\bar{\nu}$ (3 yr)	33.8	10.6	0.7	5.0	16.3

The NOνA far detector will begin taking beam from the upgraded NuMI facility in May of 2013. At this time and estimated 5 kt of detector mass will be operational and the experiment will begin integrating exposure on the detector with the 320 kW NuMI beam. Over the first six month period the beam power will be increased to 700 kW in parallel to additional blocks of the far detector being brought online. The full detector mass is estimated to be reached in March of 2014 and in May of 2014 the NuMI beam will be switched from the forward horn current to reverse horn current configuration in order to switch from the neutrino beam configuration to the anti-neutrino configuration. The sensitivity of NOνA to the ν_e and $\bar{\nu}_e$ appearance signatures are shown in Fig. 4 for the first three years of the experiment.
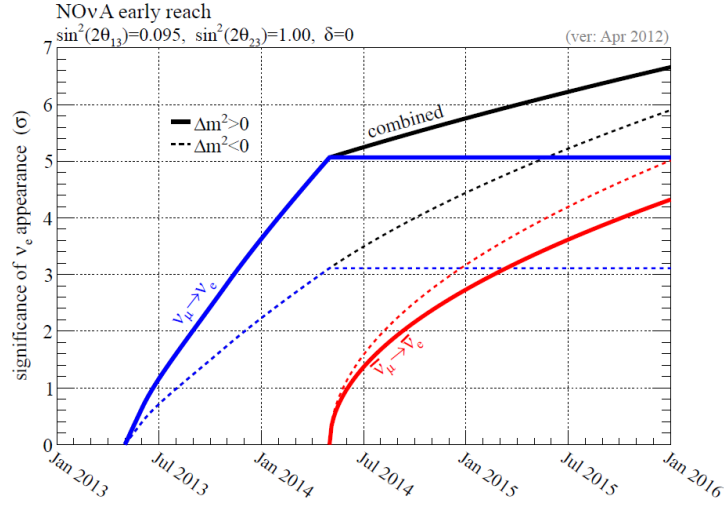

Figure 4: NOνA sensitivities to ν_e and anti-ν_e appearance as a function of time time for the first three years of running. Sensitivities assume a May 2013 start of data taking with the NuMI beam in the 320 kW forward horn current configuration (neutrino running) followed by a ramp up in beam power to 700 kW over six months. The NuMI beam configuration is assumed to switch to the reverse horn current configuration after one year.

Over these time periods NOνA will measure separately the oscillation probabilities $P(\nu_\mu \to \nu_e)$ and $P(\bar{\nu}_\mu \to \bar{\nu}_e)$ at a central energy of 2 GeV. The transition probabilities for these processes in the full three flavor oscillation analysis and in the presence of matter can be expressed as,

$$P(\overset{(-)}{\nu}_\mu \to \overset{(-)}{\nu}_e) \approx \sin^2 2\theta_{13} \sin^2\theta_{23} \frac{\sin^2(A-1)\Delta}{(A-1^2)}$$

$$\overset{(+)}{-} 2\alpha \sin\theta_{13} \sin\delta_{CP} \sin 2\theta_{12} \sin 2\theta_{23} \frac{\sin A\Delta}{A} \frac{\sin(A-1)\Delta}{A-1} \sin\Delta$$

$$+ 2\alpha \sin\theta_{13} \cos\delta_{CP} \sin 2\theta_{12} \sin 2\theta_{23} \frac{\sin A\Delta}{A} \frac{\sin(A-1)\Delta}{A-1} \cos\Delta \qquad (3.1)$$

Where:

$$\alpha = \frac{\Delta m_{21}^2}{\Delta m_{31}^2} \quad \Delta = \Delta m_{31}^2 \frac{L}{4E} \quad A = \overset{(-)}{+} G_f N_e \frac{L}{\sqrt{2}\Delta} \tag{3.2}$$

and the contribution of the sub-dominate oscillation has been suppressed. Equation 3.1 explicitly demonstrates the dependence of each of these rates on the CP-violating phase δ_{CP} as well as the sign of Δm_{13}^2. By choosing a value for Δm_{13}^2 and running δ_{CP} from 0 to 2π, the neutrino and anti-neutrino oscillation probabilities can be plotted against each other parametrically in δ_{CP} for the NOνA energy and baseline. This procedure forms allowed ellipses in the bi-probability space against which the experimental values can be compared. In the case of maximal mixing, $\sin^2 2\theta_{23} = 1$, for the NOνA baseline and central energy of 2 GeV these ellipses are shown in Fig. 5a. The sensitivity that NOνA has to resolving the mass hierarchy can then be examined by testing a given point on the ellipses corresponding to a value of δ_{CP}. Figure 5b shows a test point for $\delta_{CP} = 3\pi/2$ in the normal mass hierarchy as well as the 1σ and 2σ sensitivity contours for the test point. If NOνA were to measure $P(\nu_\mu \to \nu_e)$ and $P(\bar{\nu}_\mu \to \bar{\nu}_e)$ at the values of the test point, then the measurement would conclude that the inverted mass hierarchy is disfavored at better than the 90% confidence interval.
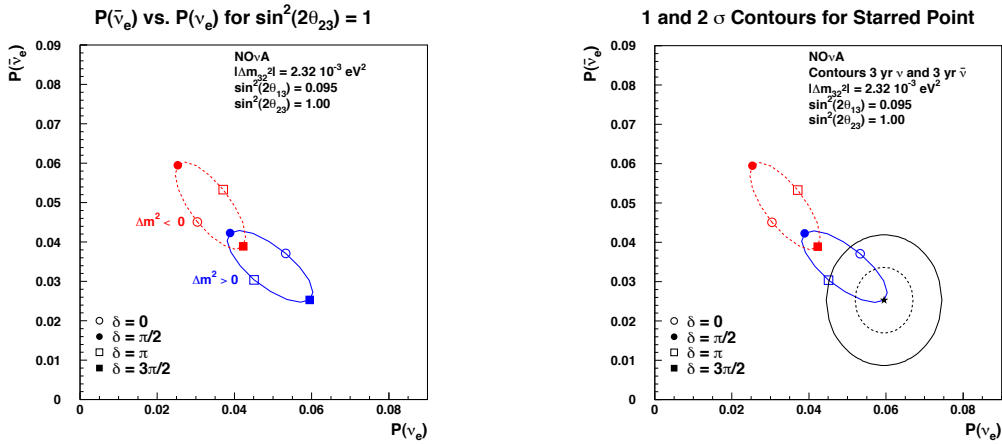

(a) Bi-probability ellipses for the normal (blue) and inverted (red) mass hierarchies assuming maximal mixing and the NOνA baseline and energy profile.

(b) The starred point represents and example NOνA measurement for the ν_e and $\bar{\nu}_e$ oscillation probabilities corresponding to $\delta_{CP} = 3\pi/2$. The black lines represent the 1σ and 2σ contours on the measurements.

Figure 5: NOνA bi-probability plots for $\sin^2 2\theta_{13} = 0.095$.

This procedure can be run for all points on the curves in Fig. 5 to map out the significance with which the experiment can resolve the mass hierarchy in both the normal and inverted cases. These sensitivities are shown in Fig. 6a for three years each of running in neutrino and anti-neutrino modes.

With $\sin^2 2\theta_{13} = 0.095$ the bi-probability ellipses for the normal and inverted hierarchy intersect each other and create an ambiguity that limits the experiment's ability in that region. This ambiguity can be broken by combining the NOνA data with similar data taken with a different
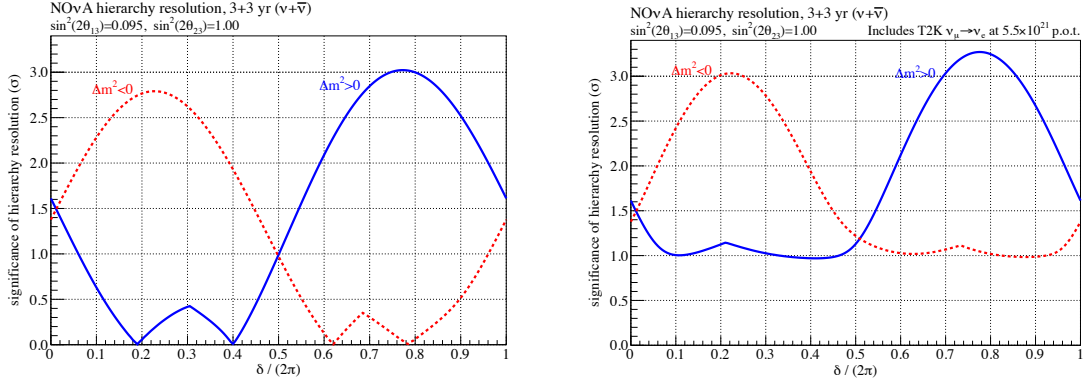
(a) NOνA sensitivities to resolution of the mass hierarchy as a function of δ_{CP}. The normal mass hierarchy is shown in blue and the inverted hierarchy in red. Values of δ_{CP} where the sensitivity goes to zero correspond to the intersection points in the bi-probability ellipses.

(b) Combined NOνA + T2K sensitivities to resolution of the mass hierarchy as a function of δ_{CP}. The combined experiments achieve 1σ significances over the full range of available δ_{CP}.

Figure 6: NOνA Sensitivities to neutrino mass hierarchy resolution

baseline or energy. By combining the NOνA data with the expected T2K sensitivities, the combined sensitivities give at least 1σ resolution of the hierarchy across the full parameter space in δ_{CP} and give better than $3\,\sigma$ resolution in the outer regions of the ellipses. These combined sensitivities are show in Fig. 6b.

Recent results from the MINOS collaboration [3] have indicated that θ_{23} may be non-maximal and currently have a best fit value that gives $\sin^2 2\theta_{23} = 0.95$. If θ_{23} is not $45°$ then the first term in Eq. 3.1, which is proportional to $\sin^2 \theta_{23}$ instead of to $\sin^2 2\theta_{23}$, causes $P(\nu_\mu \to \nu_e)$ and $P(\bar{\nu}_\mu \to \bar{\nu}_e)$ to be different for $\theta_{23} > 45°$ and $\theta_{23} < 45°$. This causes the bi-probability ellipse shown in Fig. 5 to bifurcate across the $45°$ axis, into two separate sets of solutions for the normal and inverted hierarchy. This set of possible solutions are shown in Fig. 8a for the standard NOνA parameters and a non-maximal θ_{23} consistent with the MINOS fits.

The significances of determining the octant of θ_{23}, is that in doing so we are able to determine whether the neutrino mass state ν_3 couples more to the ν_μ or ν_τ flavor states. This is shown in Fig. 7 where values of $\theta_{23} < 45°$ would indicate a greater coupling to the ν_τ state while $\theta_{23} > 45°$ would indicate a greater coupling to the ν_μ state.

NOνA's ability to distinguish the octant θ_{23} can be examined in much the same manner as the experiment's ability to resolve the mass hierarchy. The plot shown in Fig. 8b shows a test point in the measurement space which assumes a value of $\delta_{CP} = 3\pi/2$ for the case where θ_{23} is greater than $45°$. The 1σ and 2σ contours corresponding to the NOνA event rates for three years each of neutrino and anti-neutrino running. What is of particular note in this case is that the experiment is highly sensitive to the θ_{23} measurements over a very different range of δ_{CP} than that which gives the maximum sensitivity to the resolution of the hierarchy. More over NOνA's ability to resolve the θ_{23} ambiguity peaks at better than 2σ on the interval $(\pi/2, 3\pi/2)$ for the solution where $\theta_{23} < 45°$
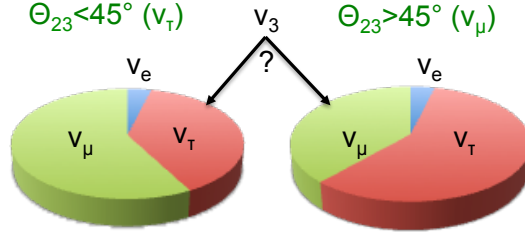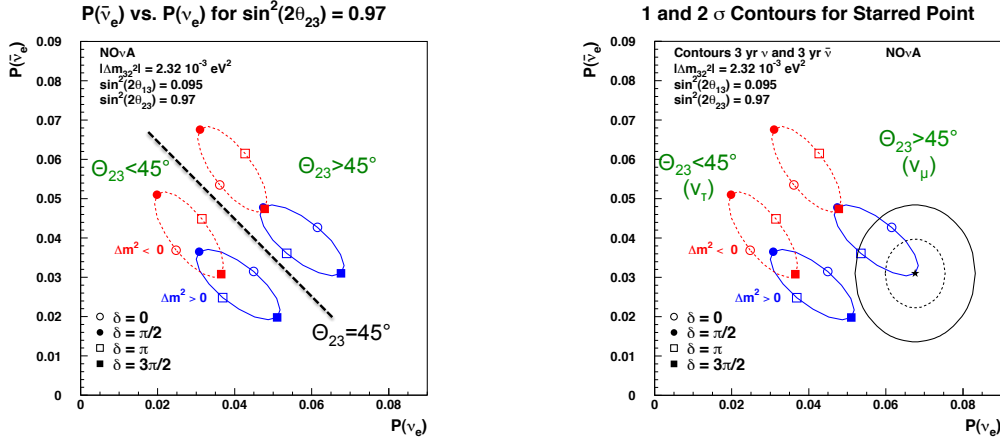
Figure 7: Relationship of ν_3 coupling to the flavor states for a non-maximal θ_{23}.

and on the interval $(0, \pi/2)$ and $(3\pi/2, 2\pi)$ for $\theta_{23} > 45°$. For these intervals there is only a weak dependence on the mass hierarchy which makes NOvA sensitive to resolving the θ_{23} octant even if it can not resolve the mass hierarchy.

(a) Bi-probability ellipses for a non-maximal θ_{23}. The bifurcation of the allowed probability curves allows for a determination of whether θ_{23} is greater or less than $45°$.

(b) Test point under the assumptions of a non-maximal θ_{23}, normal mass hierarchy and $\delta_{CP} = 3\pi/2$. The NOvA 1 and 2 sigma sensitivity contours are shown.

Figure 8: NOvA bi-probability plots for non-maximal θ_{23}, $\sin^2 2\theta_{23} = 0.095$.

4. Experiment Progress and Conclusions

With the new measures of θ_{13}, the NOvA experiment is uniquely positioned to make precision oscillations measurements that have the potential to significantly impact our knowledge of the structure of the neutrino mass hierarchy and probe for potentially large sources of CP violation in the neutrino section.

The Fermilab accelerator complex was shutdown on May 1, 2012 to undergo a year long upgrade of the facilities that will convert the recycler ring from an antiproton to a proton ring and perform other upgrades to the other complexes that will allow for the Main Injector spill cycle to

be shorted from 2.2 s to 1.33 s. During this period that NuMI target station will also be upgraded to with new targets that will support running at a 700 kW beam power.

In parallel to the accelerator upgrades, the NOνA experiment started construction of the far detector in the summer of 2012. Under the current schedule estimates, 5 kt of far detector mass will be fully operational when the FNAL beam complex turns back on in April/May 2013. At this time the beam will undergo a ramp to the full 700 kW beam power over 6 months and the NOνA detector will integrate exposure on the detector as it grows to its final mass of 15 kt in the spring of 2014. In the first six months this is expected to result in an integrated exposure of approximately 1 kt MW yr as shown in Fig. 9 and permit observation of the $\nu_\mu \to \nu_e$ oscillation signature with a 5σ significance.
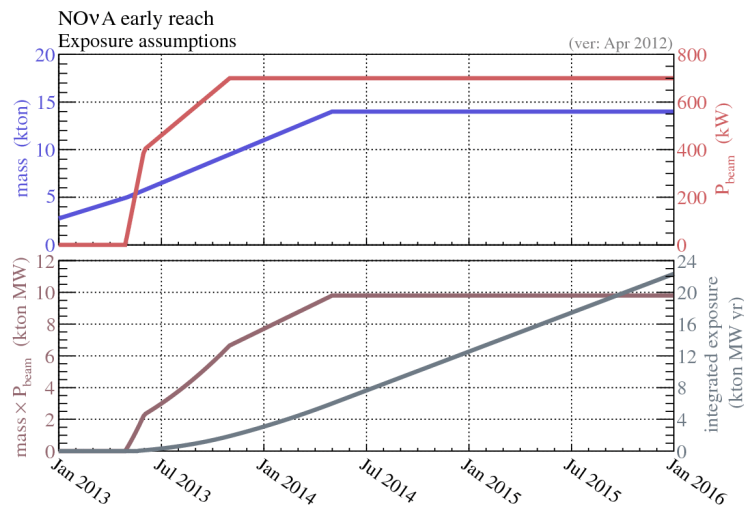

Figure 9: NOνA detector construction, beam power and integrated exposure.

References

[1] D. Forero, M. Tortola, J. Valle, *Global status of neutrino oscillation parameters after recent reactor measurements*, arXiv:1205.4018v2 [hep-ph].

[2] T. Nakaya, *Results from T2K*, talk given at Neutrino 2012, June 2012.

[3] R. Nichol, *Results from Minos*, talk given at Neutrino 2012, June 2012.

[4] F. An and others, *Observation of electron-antineutrino disappearance at Daya Bay*, arXiv:1203.1669v2 [hep-ex].

[5] S. Kim and others, *Observation of Reactor Electron Antineutrino Disappearance in the Reno Experiment*, arXiv:1204.0626v2.

[6] Y. Abe et al *Indication of reactor $\bar{\nu}_e$ disappearance in the Double Chooz Experiment*, PRL 108, 131801, (2012).